LA-UR- 97-2672

Approved for public release; distribution is unlimited.

Title: QUANTUM SPIN FLUCTUATIONS IN QUASI-ONE-DIMENSIONAL CHLORINE-BRIDGED PLATINUM COMPLEXES

CONF-970706--

Author(s): X. Wei
R.J. Donohoe
W.Z. Wang
A.R. Bishop
J.T. Gammel

Submitted to: SPIE 1997 San Diego, Conference 3145

Los Alamos
NATIONAL LABORATORY

DISCLAIMER

Quantum spin fluctuations in quasi-one-dimensional chlorine-bridged platinum complexes

X. Wei, R. J. Donohoe, W. Z. Wang, A. R. Bishop, and J. T. Gammel

Los Alamos National Laboratory, Los Alamos, NM 87545

ABSTRACT

We report experimental and theoretical studies of spin dynamic process in the quasi-one-dimensional chlorine-bridged platinum complex, $[Pt^{II}(en)_2][Pt^{IV}(en)_2Cl_2](ClO_4)_4$, where *en* = ethylenediamine, $C_2N_2H_8$. The process manifests itself in collapsing of the hyperfine and superhyperfine structures in the electron spin resonance (ESR) spectrum and non-statistical distribution of spectral weight of the Pt isotopes. More surprisingly, it is activated only at temperatures below 6 K. We interpret the phenomenon in terms of quantum tunneling of the electronic spin in a strong electron-electron and electron-phonon coupling regime. This is modeled using a non-adiabatic many-body approach, in which polarons and solitons represent local spin-Peierls regions in a strongly disproportional charge-density-wave background and display intriguing spin-charge separation in the form of pinned charge and tunneling spin fluctuations.

Keywords: electron spin resonance, spin dynamics, many-body theory, quantum tunneling, M-X materials, nonadiabatic methods.

I. INTRODUCTION

Quasi-one-dimensional halide-bridged mixed-valence metal complexes (M-X) have been synthesized with a variety of metals (Pt, Pd and Ni), halogens (I, Br, Cl), equatorial ligands and counterions. [1-9] While the average oxidation state of the metals in an M-X chain is +3, this structure is unstable to a Peierls distortion: strong electron-lattice coupling leads to charge disproportionation between the metals (alternating sites tending toward +4 and +2 valences) and dimerization of the halide sublattice toward the higher valence metal sites. As a result, a strongly commensurate charge-density-wave (CDW) ground state is formed with the degree of charge disproportionation (strength of CDW) dependent upon aspects of the chemical composition and also upon environmental influences such as temperature and pressure. $[Pt^{II}(en)_2][Pt^{IV}(en)_2Cl_2](ClO_4)_4$ (where *en* = ethylenediamine, $C_2N_2H_8$), referred to hereafter as Pt-Cl, is a well known example of these complexes. [8,9] For a given composition of equatorial ligands and counterions, the strength of the CDW increases in the series Ni<Pd<Pt and I<Br<Cl, making Pt-Cl chains strong CDW materials.

Much of the interest in MX complexes is generated by the fact that they can serve as a well controlled experimental testing ground for the examination of highly correlated narrow-band electronic materials, including the low-dimensional elements of high temperature oxide superconductors (Cu-O planes and chains). Nasu and coworkers[8] have developed a half-filled, one-band Peierls-Hubbard model in which only the metal electronic structure is explicitly included whereas Bishop and coworkers[9] have developed a complementary three-quarter-filled, two-band model where both halide and metal electronic structures are included

In a previous work,[10] we have studied the LESR spectra of various isotopically enriched Pt-Cl complexes and shown that the superhyperfine (SH-F) structures are purely associated with Cl, and that the spin-1/2 defects can be better modeled as neutral solitons by a simple Hamiltonian including significant spin density over only three Cl sites. The strongly local character of the defect correlates with the strong CDW degree.

In this work, we report the observation of drastic changes, including a redistribution of intensities, linewidths, and spectral positions of the H-F as well as SH-F lines in the LESR spectrum of Pt-Cl below 6K. These changes are unlikely to be due to extrinsic defects, instead, we argue that they result from unusual spin dynamics in Pt-Cl. Our theoretical exact diagonalization calculations indeed show that there are very low energy quantum spin excitation states in Pt-Cl, which provide a plausible and novel explanation for the observed spin dynamics, corresponding to dynamical spin-charge separation in the form of local spin-Peierls distortions.

II. EXPERIMENT

(1) Materials: all isotopes were purchased from Oak Ridge National Laboratory. The ^{194}Pt was certified to have a ^{195}Pt concentration of less than 3%. The ^{37}Cl was purchased as NaCl. The samples of Pt-Cl were synthesized from the saturated aqueous perchloric acid solution of $[Pt^{II}(en)_2]^{2+}$ and $[Pt^{IV}(en)_2]^{4+}$ by the literature method[11] and recrystallized in the absence of light at around 5 °C to obtain single crystals of Pt-Cl, with a typical dimension of about $4 \times 2 \times 0.5$ mm^3. The crystals were stored below 15 °C.

(2) ESR spectroscopy: single crystals of Pt-Cl were taken from the aqueous solution, dried on a tissue paper, and oriented on a quartz capillary by means of a small amount of vacuum grease prior to insertion into a 4 mm quartz tube with a stopcock. The sample tube was evacuated for several minutes prior to placement within the cavity of an IBM (Bruker) series ER 200 X-band spectrometer equipped with an Oxford liquid helium cryostat. The sample was cooled to 10 K or below and a spectrum recorded. No significant signals were observed prior to irradiation. The sample was then irradiated for one hour with a 50 mW/mm^2 Ar^+ laser beam operated in the visible all-lines mode. The spectra were then recorded at various temperatures from 4 K to 300 K and at various orientations between the magnetic field and the primary crystal axis, which was identified as the chain axis by examination with an analyzer.

III. EXPERIMENTAL RESULTS

The comparative LESR spectra of ^{N}Pt-^{N}Cl and ^{194}Pt-^{N}Cl (where N denotes natural abundance) at 10 K are shown in Figure 1 (see ref. 10 for more details and ref. 7 and ref. 12-18 for related studies). The ^{N}Pt-^{N}Cl spectrum exhibits a five-line hyperfine (H-F) structure with approximately 180 Gauss splitting and intensity ratio of 1 : 8 : 18 : 8 : 1, and 16 Gauss spaced syperhyperfine (SHF) structures. The signal has been assigned to spin-1/2 neutral solitons localized on two equivalent Pt sites. The H-F intensity pattern was attributed to the probability of finding the total nuclear spin moment I_z of the two Pt at -1, -1/2, 0, 1/2, and 1, respectively, which yields the observed result because natural Pt consists of 33.7% ^{195}Pt with nuclear spin 1/2 and 66.3% Pt isotopes with no nuclear spin.[7] By contrast, the ^{194}Pt-^{N}Cl spectrum, as expected, shows only a single H-F line with a linewidth of ~ 108 Gauss. We have also shown that the 16 Gauss spaced SHF structures was due to the bridging chlorines. Moreover, no motional narrowing or collapse of the ESR spectrum is observed at any temperature from 10 K to near 200 K for both ^{N}Pt-^{N}Cl and ^{194}Pt-^{N}Cl, consistent with the idea that such localized solitons in strong CDW materials should be quite immobile (strongly pinned).[19]

Drastic changes in the LESR spectrum of ^{N}Pt-^{N}Cl were, however, observed from 10 K to 4 K, as shown in Figure 2. At 4 K, no SH-F structure was observed under our normal measuring condition (modulation frequency and microwave power dependencies are discussed below). The integrated intensity for the five H-F lines at 4K changes from 1 : 8 : 18: 8: 1 to 0.7 : 17.7 : 17 : 16.5 : 0.7±0.2, where the intensity units of the 10 K spectrum are preserved. Note that the two I_z=±1/2

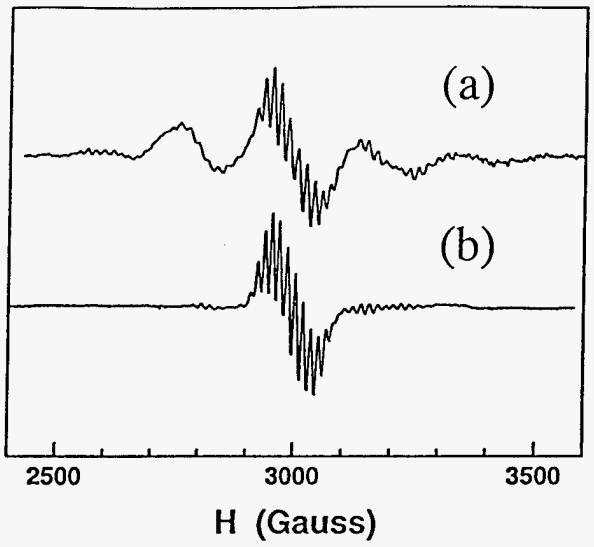

Figure 1: The comparative spectra of (a) $^{N}Pt\text{-}^{N}Cl$, and (b) $^{194}Pt\text{-}^{N}Cl$ at T = 10 K.

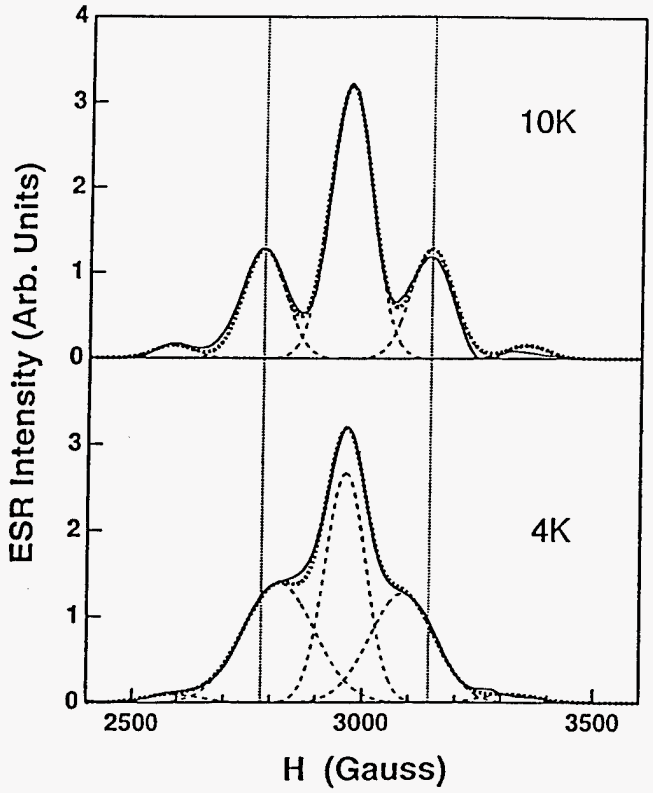

Figure 2: Comparative $^{N}Pt\text{-}^{N}Cl$ LESR spectra at 4 K and 10 K, respectively. The solid lines are experimental data, the dashed lines are the five Gaussian components for each temperature respectively, and the dotted lines are the resultant fits.

H-F lines gain intensity dramatically (more than doubled) while the other three lines lose a relatively small amount of intensity from 10 K to 4 K. The overall spectral intensity increases by nearly 50 %. Moreover, the linewidths of the five H-F lines change from an approximately uniform value of 108 Gauss at temperatures above 6 K to 94, 184, 103, 184, 94 Gauss at 4 K. Finally, the separation between the two $I_Z=\pm 1/2$ H-F lines decreases from 360 Gauss to 260 Gauss, while the other lines remain comparatively, but not perfectly (*vide infra*), fixed.

Since the aforementioned "normal" 1 : 8 : 18 : 8 : 1 hyperfine intensity pattern in $^{N}Pt\text{-}^{N}Cl$ represents the statistical distribution of Pt isotopes, one might naturally assume that deviation from this distribution is due to the sudden appearance of an unrelated defect which contributes to the excess spectral weight. [18] Accordingly, the 4 K LESR spectrum of $^{194}Pt\text{-}^{N}Cl$ would be expected to reveal this new defect more cleanly because there is no interference from the $I_Z=\pm 1/2$ H-F lines in $^{194}Pt\text{-}^{N}Cl$. Figure 3 shows the low temperature dependence of the ESR spectrum for $^{194}Pt\text{-}^{N}Cl$. It is striking that there is no counterpart in the 4 K $^{194}Pt\text{-}^{N}Cl$ spectrum to the increased spectral weight in the analogous spectrum of $^{N}Pt\text{-}^{N}Cl$. Thus, if such a "new" defect exists, it would be selectively localized on only the ^{195}Pt (I=1/2) sites and be totally absent in $^{194}Pt\text{-}^{N}Cl$. This is a quite implausible scenario. Figure 3 also shows that the SH-F structure is largely suppressed at 4 K and appears quite suddenly when the temperature is raised from 4 to only 6 K. In fact, the spectrum at 4 K is distinct from that at 6 K in several ways. Quite unexpected is the observation that the bandwidth is more narrow by ~ 17 G at 4 K. In addition, there is a slight shift (Δg ~ 0.001) of the spectrum. In comparison, the spectral profile remains relatively unchanged from 6 to 70 K. Moreover, the rapid change in the overall width and g value of the $^{194}Pt\text{-}^{N}Cl$ LESR spectrum at low temperatures is also consistent with the $^{N}Pt\text{-}^{N}Cl$ results where the central H-F line corresponding to $I_Z=0$ also narrows and shifts at 4 K (Figure 2). To again consider the possibility that these two spectra represent the presence of unrelated defects, i.e., the spectrum at 4 K represents one defect and the excess spectral weight in the 6 K spectrum represents another, we studied the LESR spectrum after annealing the sample between 4 K and higher temperatures (near 80 K) and found that even though the overall intensity is decreased by more than 35% after the annealing, the 4 K and 6 K spectra retain the same relative intensities. The possibility that two defects with superimposed spectra experience identical annihilation with raised temperatures is not credible. Thus, we conjecture that the spectral variations between 4 and 6 K are associated with a single type of defect.

Below 10K, temperature dependence of the spectral intensity in $^{194}Pt\text{-}^{N}Cl$ deviates from $\tanh(\mu B/2kT)$, which can be derived from the two-level Boltzmann distribution.[20] This indicates that the spin relaxation rate is sufficiently reduced and microwave saturation effects may be significant. We found that variations of the modulation frequency and microwave power at 4 K indeed affect the spectrum in a manner similar to raising the temperature to 6 K. In $^{194}Pt\text{-}^{N}Cl$, where the SH-F lines are not resolved at 4 K under typical measurement conditions (modulation frequency = 100 kHz; microwave power = 2 - 20 mW), the structure becomes well resolved when measured at low modulation frequency (for example, 3 kHz) and/or reduced microwave power (for example, 2 μW). Figure 4 shows the integrated 4 K LESR spectra of $^{194}Pt\text{-}^{N}Cl$ measured at field modulation frequencies of 100 kHz and 3 kHz respectively. However, we noted that the overall width of the spectrum is narrowed when measured at higher microwave power or at higher modulation frequency. If the losing of SHF structures had resulted from line broadening due to the saturation effect, we would expect that the overall spectral width should be broadened. The fact that the 6K spectral profile can be recovered at 4K by variations in the instrumentation settings does not suggest that the fundamental defect structure has been altered by a phase transition. Therefore, the spectral narrowing at low temperatures suggests a dynamical nature, even though the saturation effect may play a role in the temperature dependence of the overall spectral intensity.

The temperature dependence of the two $I_Z=\pm 1/2$ H-F line intensities seems to follow the thermalized distribution, $\tanh(\mu B/2kT)$, at 4 K and 10 K, respectively. Furthermore, the spectrum of $^{N}Pt\text{-}^{N}Cl$ measured at low microwave power shows that the two $I_Z=\pm 1/2$ H-F lines are less broadened and less intense, relatively, as compared with the spectrum measured at high microwave power, similar to the changes with raising the sample temperature. This indicates that the microwave

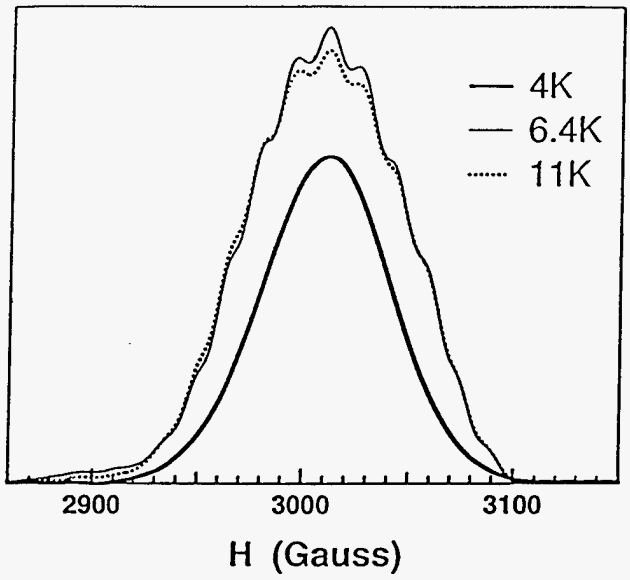

Figure 3: Temperature dependence of the ^{194}Pt-NCl LESR spectrum at $g_{\perp}$. The spectrum undergoes dramatic changes from 4 to 6.4 K, and remains relatively unchanged between 6.4 and 11 K.

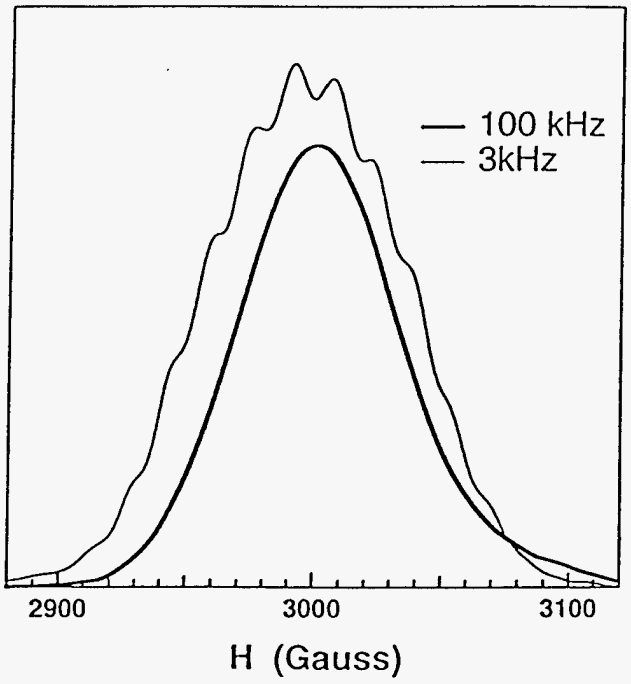

Figure 4: The comparative LESR spectra of ^{194}Pt-NCl measured with field modulation frequencies of 100 kHz and 3 kHz.

saturation effects are less significant in affecting the overall intensity of the two $I_Z=\pm1/2$ H-F lines than the central $I_Z=0$ H-F line, i.e., the spin relaxation rates depend on I_Z. Therefore, the apparent "abnormal" and non-statistical H-F line intensity distribution is due to I_Z-dependent spin relaxations. On the other hand, the broadening and collapsing of the two $I_Z=\pm1/2$ H-F lines in $^{N}Pt\text{-}^{N}Cl$ is consistent with the broadening and collapsing of the SH-F structures on the central $I_Z=0$ H-F lines in $^{N}Pt\text{-}^{N}Cl$ as well as in $^{194}Pt\text{-}^{N}Cl$. This suggests that the spin dynamics occur at both Pt and Cl sites.

IV. DISCUSSION AND MODELING

The above spectral changes of the H-F structure, which is associated with Pt nuclei, and the SH-F structure, which is associated with Cl nuclei, at low temperatures are quite unusual. The intensity pattern of 0.7 : 17.7 : 17 : 16.5 : 0.7 (±0.2) at 4 K is especially puzzling because no obvious configuration can yield such an intensity pattern in accord with the statistical distribution of the Pt isotopes. Yet, as argued above, these changes are unlikely to be due to the emergence of new defects, phase transitions, or saturation effects. Therefore, the spectral changes observed between 4 and 6 K are apparently a manifestation of a dynamic process. Because the intensities of the LESR spectra observed upon cycling between 4 and 6 K are reproducible, any dynamics are apparently localized and do not lead to activation or annihilation of the defect. Sakai *et al.* [16] proposed a dynamical model to explain the observation in $^{N}Pt\text{-}^{N}Cl$ that the SH-F lines are present in the $I_Z=0$ and ±1 H-F lines and absent in the $I_Z=\pm1/2$ H-F lines. In their model, the spin density of neutral solitons are fluctuating back and forth around the equilibrium position. However, in such a situation one would also expect the overall linewidths of the two $I_Z=\pm1/2$ lines to be broader than the other three H-F lines, which is not in agreement with the LESR spectra at temperatures higher than 6 K. Below 6 K, the two $I_Z=\pm1/2$ lines do indeed broaden and collapse toward the central $I_Z=0$ line from 6K to 4K. In this instance, the classical Anderson spin-exchange narrowing model[21] can be investigated for applicability:

$$[\Delta H_{12}(0)]^2-(\Delta H_{12})^2=2(\Gamma-\Gamma_0)^2 \qquad (1)$$

where the resonant lines are at fields H_1 or H_2 with $\Delta H_{12} = H_2 - H_1$, Γ_0 is the intrinsic linewidth, Γ is the measured linewidth and $\Delta H_{12}(0)$ is the intrinsic splitting without spin-exchange. However, the values extracted from Figure 2, i.e., $\Delta H_{12}(0) = 360$ Gauss, $\Delta H_{12} = 270$ Gauss, $\Gamma_0 = 108$ Gauss, and $\Gamma = 184$ Gauss, are not in accord with Equation (1). In general, any simple dynamical model is not likely to explain the low temperature phenomenon in Pt-Cl. In fact, the data provide a surprising indication that the dynamic phenomenon is not evenly applied among the isotopically distinct defect sites: broadening and collapsing for the lines and narrowing for the line.

To explain the unusual spin dynamics, we propose that we need to consider that Pt-Cl is a non-conventional CDW system, in which strong electron-phonon (*e-ph*) coupling dominates and that the CDW ground state is accompanied by a nearly degenerate state due to quantum tunneling through the CDW barrier between the two equivalent minima in the adiabatic potential. This kind of quantum tunneling involves only charges and phonon excitations instead of spin excitations. However, the strong electron-electron (*e-e*) correlations in Pt-Cl play an important role in determining its electronic dynamics. Therefore, theoretical calculations for such CDW systems need to overcome the difficulty in proper handling of *e-e* correlations as well as *e-ph* couplings, which are usually treated adiabatically. In non-adiabatic treatments, the effect of quantum lattice fluctuations is taken into account along with high-order contributions from the *e-ph* couplings. Then, the quantum magnetic fluctuations, favored by the *e-e* correlations, can be delicately mixed into the CDW long-range order induced by the *e-ph* couplings.

To quantify these considerations, we study here a Peierls-Hubbard system of strongly correlated electrons and phonons governed by *e-e* interactions and *e-ph* couplings. [22] The system Hamiltonian can be written as:

$$
\begin{aligned}
\mathcal{H} = & \sum_{i,\sigma} \left[-t_0 + \alpha_i (b_i^\dagger + b_i) - \alpha_{i+1} (b_{i+1}^\dagger + b_{i+1}) \right] (c_{i\sigma}^\dagger c_{i+1\sigma} + \text{H.c.}) \\
& + \sum_{i,\sigma} \left[e_i - \beta_{i-1} (b_{i-1}^\dagger + b_{i-1}) - \beta_{i+1} (b_{i+1}^\dagger + b_{i+1}) \right] c_{i\sigma}^\dagger c_{i\sigma} \\
& + \sum_i U n_{i\uparrow} n_{i\downarrow} + \sum_{i,\sigma\sigma'} V n_{i\sigma} n_{i+1\sigma'} \\
& + \sum_i \left[\hbar\omega_i (b_i^\dagger b_i + \frac{1}{2}) - \kappa_{i,i+1} (b_i^\dagger + b_i)(b_{i+1}^\dagger + b_{i+1}) \right] ,
\end{aligned}
\tag{2}
$$

where t_0 and e_i are the electronic hopping integral and on-site energy, respectively, while U and V are the Hubbard *e-e* interactions. α_i and β_i are the inter-site and off-site *e-ph* coupling constants, respectively. $\hbar\omega_i$ is the bare phonon energy at site i, while $\kappa_{i,i+1}$ is the lattice coupling between sites i and $i+1$. We adopted the parameter set based in Ref. 22. Since the coherent lengths of quantum spins and lattice distortions are very short in Pt-Cl, due to strong *e-ph* and *e-e* interactions, it is sufficient to only consider a finite chain. The model systems that we studied for Pt-Cl include: (1) a five-lattice-site system with three Cl atoms, two Pt atoms and eight valence electrons, which corresponds to a neutral Pt-Cl chain; (2) a similar seven-site system; (3) a five-site system with one isotopic ^{195}Pt atom among other ^{194}Pt atoms; and (4) a five-site system with one doped electron. A free boundary condition was adopted here.

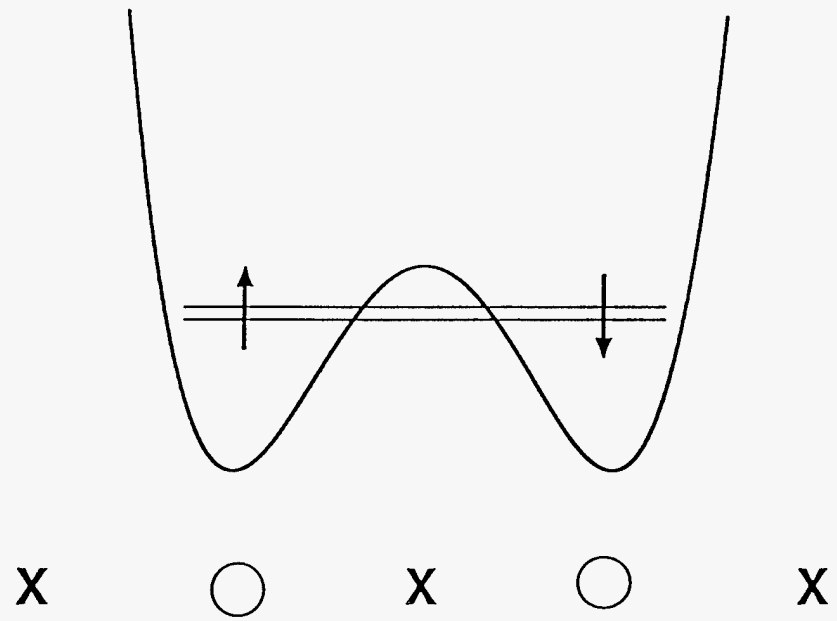

Figure 5: The schematic diagram for the five-lattice-site system with three Cl atoms (X), two Pt atoms (oval) and eight valence electrons.

To solve this system without an adiabatic approximation and other approximations related to the *e-e* interactions, we use the exact diagonalization scheme developed in our previous studies of quantum phonons[23] and *e-ph* coupled systems.[24] In this way, the effects of *e-ph* coupling and *e-e* correlations can be fully accounted for on the finite chains.

Our goal is to reveal dynamic responses of electrons and phonons in different channels of excitations. To this end, we calculated three time-dependent correlation functions defined on the ground state of the system, $|g\rangle$:

(a) charge density Green's function (GF): $f(t) = \langle g|\sum_i n_i(0)n_i(t)|g\rangle$;

(b) spin-spin GF: $s(t) = \langle g|\sum_i s_i^z(0)s_i^z(t)|g\rangle$;

(c) phonon-phonon GF: $p(t) = \langle g|\sum_i u_i(0)u_i(t)|g\rangle$;

where n_i, s^z_i and u_i are the electronic operators of charge density, the z-component of spins and the phonon displacement operator, respectively. The basic results are similar for all the above configurations. The calculated Fourier transformations of the GF's for the neutral five-site chain are shown in Table 1.

ω	f(ω)	ω	s(ω)	ω	p(ω)
0.00	0.90	3.7×10^{-5}	0.90	5.4×10^{-3}	0.08
0.83	0.04	2.90	0.27	2.4×10^{-2}	0.01
2.90	0.41	2.91	0.10	0.05	0.90

TABLE 1. The lowest peak positions in the Fourier transformed spectra of the Green's functions (ω in eV, the spectral weight in arbitrary units).

In Table 1, we notice the different responses in the three channels, which indicates the differences upon charge, spin or phonon excitations. The electronic degrees of freedom of charges and spins have different time-dependencies because of the strong correlations between electrons and phonons. In the charge channel, the poles of the GF indicates the dynamics due to the quantum tunneling within the ground state, and the charge excitations across the Hubbard gap, while in the phonon channel, there are excitations corresponding to the single and multi-phonon states. Within the channel of spin excitations, along with higher spin excitations, there exists an excitation with energy of 0.04 meV in the lowest part of the spectrum. This is a pure spin excitation because no charge response can be found in this region. This separation between the degrees of freedom of spin and charge comes from the mixing of magnetic fluctuations into the CDW ground state and the first excited state. Without the inclusion of the non-adiabatic contributions from the *e-ph* couplings, this separation cannot be revealed. Comparing the wavefunctions of this spin excited states to the ground state, we notice that the change mainly comes from the components of the electronic states which have single electron occupations.

The local quantum electronic spin fluctuation will affect the ESR spectrum in several ways:

1. The quantum electronic spin fluctuation will cause the nuclear spin of ^{195}Pt and the bridging Cl to flip its moments through the anisotropic hyperfine interactions. Because the resonant magnetic field, H, of the five H-F lines in $^{N}Pt\text{-}^{N}Cl$ depends on the total nuclear spin moment I_Z of the two Pt sites being -1, -1/2, 0, 1/2, 1, respectively. Flipping the nuclear spins of Pt will lead to the dynamical exchange of these H-F lines. In particular, the spin fluctuation will shift the I_Z = -1/2 line to the I_Z =1/2 line, and vice versa. This creates a dynamical spin exchange mechanism similar to the classical Anderson model and cause the two $I_Z = \pm 1/2$ lines to broaden and collapse toward each other. On the other hand, the I_Z = 0 line predominantly arises from Pt dimers with the nuclear spin of each Pt being 0 (i.e., non ^{195}Pt); and the electron spin fluctuation on the zero-spin Pt sites will have no effect on the I_Z = 0 H-F line. However, the electron spin fluctuation on the bridging Cl sites will lead to the collapsing of the SH-F structures and narrowing of the overall linewidth of the I_Z = 0 H-F line.

2. We observed that the temperature dependence of the overall ESR intensity at 10 K and 4 K does not follow the two-level thermal distribution and shows some degree of power saturation at 4 K. However, the saturation effect is more pronounced for the I_Z = 0 H-F line and much less for the two $I_Z = \pm 1/2$ lines. The saturation effect is expected at low temperatures when spin lattice relaxation time T_1 becomes very long. For the two $I_Z = \pm 1/2$ lines, however, the dynamical exchange will activate a new channel for spin relaxation and thus the saturation effect is ameliorated at low temperatures. This explains the non-statistical H-F intensity distribution at 4 K and the microwave power and modulation frequency dependence. I_Z dependent spin relaxation times, both T_1 and T_2, have been observed in many systems. However, we believe that our current study provides a new example with a distinctive mechanism for the phenomenon.

3. Because the tunneling levels are closely packed, thermal distribution of states among the levels at higher temperatures will lead to the averaging of electron spin on Pt and Cl sites and deactivate the dynamical spin fluctuation. Thus we expect that a "normal" ESR spectrum will be observed at temperatures above 6 K.

V. SUMMARY

The LESR spectra of Pt-Cl at temperatures above 6K are consistent with a neutral soliton model. Below 6K, a redistribution of intensities, linewidths, and spectral positions of the H-F as well as SH-F lines were observed: (1) the H-F line intensities no longer follow the Pt isotope statistics; (2) spectral broadening was observed in some H-F lines and narrowing was observed in some other H-F lines; and (3) spectral collapsing of some H-F and SH-F lines were observed. It is unlikely that these changes are due to additional defects. Some very low energy quantum spin excitation states in Pt-Cl, corresponding to local spin-Peierls tunneling in astrong CDW background, were revealed by our nonadiabatic model calculations, which provide a plausible and novel explanation for the observed spin dynamics.

V. ACKNOWLEDGMENTS

We would like to thank B. I. Swanson, S. Johnson, and A. Saxena for useful discussions. Work at LANL was supported by the Laboratory Directed Research and Development fund as an award to R.J.D, and as a Director's Postdoctoral support award to X.W.

REFERENCES

1. H. J. Keller, in *Extended Linear Chain Compounds*, edited by J. S. Miller (Plenum, New York, 1983), vol. 1, p. 357.
2. N. Kuroda, M. Sakai, Y. Nishima, M. Tanaka, and S. Kurita, Phys. Rev. Lett. 58, 2122 (1987).
3. H. Okamoto, T. Mitani, K. Toriumi, and M. Yamashita, Phys. Rev. Lett. 69, 2248 (1992).

4. R. J. H. Clark, in *Advances in Infrared and Raman Spectroscopy*, edited by R. J. H. Clark and R. E. Hester (Wiley Heyden, New York, 1984), Vol. 11, p. 95, and references therein.
5. L. DeGiorgi, P. Wachter, M. Haruki, and S. Kurita, Phys. Rev. B **40**, 3285 (1989); *ibid*,**42**, 4341 (1990).
6. T. Kobayashi, H. Ooi, and M. Yamashita, Mol. Cryst. Liq. Cryst. 256, 847 (1994).
7. A. Kawamori, R. Aoki, and M. Yamashita, J. Phys. C **18**, 5487 (1985).
8. A. Mishima and K. Nasu, Phys. Rev. B **39**, 5758 (1989); ibid, **39**, 5763 (1989).
9. J. T. Gammel, A. Saxena, I. Batistic, A. R. Bishop, and S. R. Phillpot, Phys. Rev. B **45**, 6408 (1992); S. M. Weber-Milbrodt, J. T. Gammel, A. R. Bishop, and E. Y. Loh, Phys. Rev. B **45**, 6435 (1992); I. Batistic, X. Huang, A. R. Bishop, and A. Saxena, Phys. Rev. B **48**, 6065 (1993).
10. X. Wei, S. R. Johnson, B. I. Swanson, R. J. Donohoe, Phys. Rev. B (in press).
11. S. C. Huckett, R. J. Donohoe, L. A. Worl, A. D. F. Bulou, C. J. Burns, J. R. Laia, D. Carrol, and B. I. Swanson, Chem. Mat. **3**, 123 (1991).
12. S. Kurita and M. Haruki, Synth. Met. **29**, F129 (1989).
13. N. Kuroda, M. Sakai, M. Suezawa, Y. Nishina, and K. Sumino, J. Phys. Soc. Jpn. **59**, 3049 (1990).
14. N. Kuroda, M. Sakai, M. Suezawa, Y. Nishina, K. Sumino, and M. Yamashita, Mol. Cryst. Liq. Cryst. **216**, 169 (1992).
15. C. A. Arrington, C. J. Unkefer, R. J. Donohoe, S. C. Huckett, S. Kurita, and B. I. Swanson, Solid State Commun. **84**, 979 (1992).
16. M. Sakai, N. Kuroda, M. Suezawa , Y. Nishina, K. Sumino, and M. Yamashita, J. Phys. Soc. Jpn. **61**, 1326 (1992).
17. N. Kuroda, M. Ito, Y. Nishina, A. Kawamori, Y. Kodera, and T. Matsukawa, Phys. Rev. B **48**, 4245 (1993).
18. S. Ota and S. Kurita, Mol. Cryst. Liq. Cryst. **256**, 879 (1994).
17. S. Kurita, M. Haruki, and K. Miyagawa, J. Phys. Soc. Jpn. **57**, 1789 (1988).
18. N. Kuroda, M. Nishida, and M. Yamashita, Phys. Rev. B **52**, 17084 (1995) This study is of the BF_4 analogue of the ClO_4 Pt-Cl complex.
19. Y. Onodera, J. Phys. Soc. Jpn **56**, 250 (1987).
20. N. M. Atherton, *Principles of Electron Spin Resonance* (Ellis Horwood and Prentice Hall. 1993).
21. P. W. Anderson, J. Phys. Soc. Jpn **9**, 316 (1954).
22. J. T. Gammel, A. Saxena, I. Batistic, A. R. Bishop, and S. R. Phillpot, Phys. Rev. **B45**, 6408 (1992).
23. W. Z. Wang, J. T. Gammel, A. R. Bishop and M. I. Salkola, Phys. Rev. Lett. **76**, 3598 (1996).
24. W. Z. Wang, J. T. Gammel and A. R. Bishop, (unpublished).

DoE

(18) DoE, XF
(19) UC-900, DOE